DE GRUYTER OPEN

Nova Biotechnol Chim (2017) 16(1): 32-41
DOI: 10.1515/nbec-2017-0005

Nova Biotechnologica *et* Chimica

Imaging of photoassimilates transport in plant tissues by positron emission tomography

Denisa Partelová[a], Klára Kuglerová[a], Yevheniia Konotop[b], Miroslav Horník[a,✉], Juraj Lesný[a], Marcela Gubišová[c], Jozef Gubiš[c], Peter Kováč[a,d] and Ildikó Matušíková[a]

[a] *Department of Ecochemistry and Radioecology, Faculty of Natural Sciences, University of SS. Cyril and Methodius in Trnava, Nám. J. Herdu 2, Trnava, SK-917 01, Slovak Republic*

[b] *Department of Plant Biology, Educational and Scientific Center "Institute of Biology and Medicine", Taras Shevchenko National University of Kyiv, Volodymyrska 64, Kyiv, 016 01, Ukraine*

[c] *Plant Production Research Institute, National Agricultural and Food Centre, Bratislavská cesta 122, Piešťany, SK-921 68, Slovak Republic*

[d] *BIONT Inc., Karloveská 63, Bratislava, SK-842 29, Slovak Republic*

Article info

Article history:
Received: 15th December 2016
Accepted: 15th June 2017

Keywords:
2-[^{18}F]FDG
PET
Photoassimilates
Transport
Plant tissues
Giant reed

Abstract

The current findings show that positron emission tomography (PET), primarily developed for medical diagnostic imaging, can be applied in plant studies to analyze the transport and allocation of wide range of compounds labelled with positron-emitting radioisotopes. This work is focused on PET analysis of the uptake and transport of 2-deoxy-2-fluoro[^{18}F]-D-glucose (2-[^{18}F]FDG), as a model of photoassimilates, in tissues of giant reed (*Arundo donax* L. var. *versicolor*) as a potential energy crop. The absorption of 2-[^{18}F]FDG and its subsequent transport in plant tissues were evaluated in both acropetal and basipetal direction as well. Visualization and quantification of the uptake and transport of 2-[^{18}F]FDG in plants immersed with the root system into a 2-[^{18}F]FDG solution revealed a significant accumulation of ^{18}F radioactivity in the roots. The transport rate in plants was increased in the order of plant exposure through: stem > mechanically damaged root system > intact root system. PET analysis in basipetal direction, when the plant was immersed into the 2-[^{18}F]FDG solution with the cut area of the leaf of whole plant, showed minimal translocation of 2-[^{18}F]FDG into the other plant parts. The PET results were verified by measuring the accumulated radioactivity of ^{18}F by direct gamma-spectrometry.

Introduction

Among the important issues that currently affect the whole world are mainly food shortage also in direct connection with climate changes and environment pollution. Plant growth and yields are dependent on photosynthetic fixation of carbon, and optimal allocation of carbon to growing sink tissues (Karve *et al.* 2015). To achieve increase in yields on available arable land, it must be developed a mechanistic understanding of photosynthetic C-fixation, C-transport and C-allocation to different tissues, and the regulatory system that controls photosynthesis and C-allocation (Evans 2013).

Also, a long-standing aim for plant biologists is capturing and interpreting water and sugar flow in plants because of their vital importance for plant

✉ *Corresponding author:* hornik@ucm.sk

growth and life (Hubeau and Steppe 2015; Fiorani *et al.* 2012). In this way, non-invasive imaging methods that analyze the photoassimilates transport and allocation in plants on appropriate spatial and temporal scales can play an important role. It is generally known and accepted that radiotracer imaging is one of the few methods that enable to study and analyze the dynamics of substances in a living plant body, without sampling or fixation of plant tissues (Kawachi *et al.* 2016). One of these radiotracer imaging systems and approaches is positron emission tomography (PET).

PET represents a non-invasive *in vivo* and *real-time* imaging technique that can achieve spatial resolution on the order of millimetres and provides quantitative information about dynamic physiological processes over a relatively large field of view (Karve *et al.* 2015). Such systems have been developed to give the medical world a tool to measure the activity of organs, cell aggregates, or brain zones, and primarily for the diagnosis of human cancer diseases. In addition to these biomedical or medical diagnosis applications, PET can be used to study the regulation of plant growth and development *via* metabolites transport (Karve *et al.* 2015). The most frequently used PET positron emitters are carbon-11 (^{11}C), nitrogen-13 (^{13}N), oxygen-15 (^{15}O), and fluorine-18 (^{18}F) due to their short half-lives between 3 and 110 min (McRae *et al.* 2009). The radiotracers, i.e. labelled molecules with positron emitters, are absorbed *via* normal metabolism and distributed throughout the plant body. *In vivo* PET analysis involves the γ-rays detection after annihilation process of an emitted positron with a nearby electron producing two 511 keV photons and enables to track the transport and distribution of the radiotracers in the plant as a function of time (Kiser *et al.* 2008). For plant biologists, the advantages of PET systems mainly include the capability of providing *real-time* dynamic images of positron-emitting isotopes or the movement of labelled molecules under *in vivo* conditions without damage to the plants, the possibility to obtain 3D images, and measurements in absolute units of radioactivity with high precision.

The previous papers (Partelová *et al.* 2014; 2016) deal with the evaluation of application potential of a commercial microPET system in visualization and quantification of uptake and transport of 2-deoxy-2-fluoro[^{18}F]-D-glucose (2-[^{18}F]FDG) within the tissues of tobacco plants (*Nicotiana tabacum* L.) showing very thin anatomical structures. Discussed are also the effects of various factors (including the design of experiments, initial conditions of experiments, and the morphological and physiological parameters of plants or plant organs) on visual or quantitative side of the obtained 3D PET images in connection with the distribution of 2-[^{18}F]FDG within the plant tissues.

A radioactive 2-[^{18}F]FDG is a chemical analogue of D-glucose (substitution of OH for F at the C-2 position), but only in terms of the transport pathways of D-glucose. The 2-[^{18}F]FDG is transported across the cell membrane by D-glucose transport systems, but the metabolic fate of 2-[^{18}F]FDG will be different from D-glucose (Plathow and Weber 2008). It is commonly used in medical diagnostics and animal studies to trace the uptake and metabolism of D-glucose in metabolically active tissues, such as brain tissue or cancer cells, however is rarely used in plant imaging studies to trace sugar dynamics (Fatangare *et al.* 2014).

Giant reed (*Arundo donax* L.), belonging to *Poaceae*, is a low-maintenance, multipurpose crop providing biomass for energy, fibre, pulp and other raw materials. A typical and notable characteristic of giant reed (*A. donax* L.) plants is the storage of large amounts of carbohydrates in their root system. Currently, considering the fact that giant reed plants are tolerant to diverse soil types and even to adverse environmental conditions, such as supranormal concentration of salts, drought or low availability of nutrients, giant reed represents a fast-growing and high-yielding crop with high application potential in bioenergy (Mack 2008). It could become an important energy crop due to its high yield (the highest multiyear dry biomass production 400 t per ha) and capacity to grow in marginal land, therefore not competing with the arable land used for food production (Czakó and Márton 2010). Cultivation of giant reed has a positive energy balance and compares favourably to other biomass crops, including C4 species, because of its exceptionally high water

utilization efficiency and high photosynthetic activity at hot climate despite its C3 anatomy (Rossa *et al*. 1998). However, until challenges concerning giant reed breeding and cultivation practices as well as pollution of the environment by emission from direct combustion of giant reed will be solved, bioethanol production from lignocellulose appears to be the best way to utilise the giant reed biomass (Pilu *et al*. 2012). Moreover, properties of this crop including adaptability to high water, salinity, nutrient inputs, and tolerance to pollutants, allow phytoremediation application combined with biomass production (Czakó and Márton 2010).

The aim of this work was to visualize and quantify the uptake and distribution of 2-[^{18}F]FDG, as a model of photoassimilates, in tissues of giant reed (*A. donax* L. var. *versicolor*) plants, as a potential energy crop, by positron emission tomography. The processes of absorption of 2-[^{18}F]FDG and its subsequent transport in tissues of giant reed plants were evaluated in acropetal and basipetal direction as well.

Experimental

Seedlings of giant reed

Seedlings of giant reed (*Arundo donax* L. var. *versicolor*) were obtained by vegetative propagation under *in vitro* conditions in the following steps: (i) lateral buds were cultivated in an MS medium (Murashige and Skoog 1962) with an addition of 2–4 mg/dm^3 of BAP (6-benzylaminopurine) as a cytokinin-type growth regulator for induction of shoots development; (ii) the rooting of regenerated shoots was achieved on MS medium without an addition of growth regulators, and (iii) the pre-cultivation of giant reed seedlings before the experiments was carried out in a diluted nutrient solution (25 % strength) according to Hoagland (1920). The plants were cultivated at a photoperiod of 16 h light / 8 h dark (maximum light intensity was 11 450 lx), temperature of 28 °C (light) / 18 °C (dark) and a relative humidity of 60–80 %, which were provided by the plant growth chamber (KBWF 720; Binder, Germany). The composition of the full strength Hoagland medium (100 % HM) was (in mg/dm^3): $MgSO_4.7H_2O$ – 370; KNO_3 – 404; $CaCl_2$ – 444; $NaH_2PO_4.2H_2O$ – 292; $Na_2HPO_4.12H_2O$ – 46.5; $FeSO_4.7H_2O$ – 17.9; $NaNO_3$ – 340; NH_4Cl – 214; NH_4NO_3 – 160; H_3BO_3 – 8.5; $Na_2MoO_4.2H_2O$ – 0.06; $MnSO_4.5H_2O$ – 5.0; $ZnSO_4.7H_2O$ – 0.66; $CuSO_4.5H_2O$ – 0.8.

Production of ^{18}F and synthesis of 2-[^{18}F]FDG

Positron emitter ^{18}F ($T_{1/2}$ = 109.5 min) in the form of F^- anions was produced *via* the reaction ^{18}O (*p, n*) ^{18}F using $H_2{}^{18}O$ and the cyclotron Cyclone 18/9 (IBA, Belgium). The important intermediate 1,3,4,6-tetra-*O*-acetyl-2-[^{18}F]fluoro-D-glucopyranose for the production of 2-[^{18}F]FDG was synthesised from the precursor 1,3,4,6-tetra-*O*-acetyl-2-*O*-trifluoromethanesulfonyl-*β*-D-manno-pyranose, the phase-transfer catalyst aminopolyether-potassium complex (Kryptofix® 222) and produced [^{18}F]F^-. The final product 2-[^{18}F]FDG was obtained by the acid hydrolysis of mentioned intermediate. The production of ^{18}F and synthesis of 2-[^{18}F]FDG were carried out by the company BIONT Inc. (Bratislava, Slovak Republic). The physico-chemical parameters of the final solution of 2-[^{18}F]FDG supplemented with NaCl (9.0 g/dm^3) and produced by the mentioned procedure as radiopharmaceutical product under the trade name biontFDG are summarized in the Table 1.

The solution of 2-[^{18}F]FDG applied in experiments was diluted with deionised water at a volume ratio of 1 : 9.

Experimental setup and PET analysis

For the experiments, uniform seedlings of giant reed (*A. donax* L. var. *versicolor*) were chosen in terms of their growth phase, height (approx. 15 cm), weight (approx. 0.4 g; w.w.) and number of leaves. The visual and quantitative analysis of 2-[^{18}F]FDG uptake and distribution in tissues of giant reed plants were carried out in two experimental configurations. In the first experimental setup, the uptake of 2-[^{18}F]FDG by giant reed was evaluated in the acropetal direction by immersion of intact root system, damaged root system (cut root capillaries) or stem

Table 1. Physico-chemical parameters of produced 2-[^{18}F]FDG solution.

Analyzed parameter	Determined/Evaluated	Value/Character
Volume	Gravimetrically	0.2–0.5 cm^3
Opalescence	Organoleptically	Clear, colourless solution
pH	Colorimetrically	6.8–7.2
Specific volume radioactivity	Ionization chamber	1.6–2.8 GBq/cm^3
Half-life decay	Ionization chamber	109.5 min
Concentration of 2-[^{18}F]FDG	Liquid chromatography	< 0.0016 mg/cm^3
Kryptofix® 222 concentration	Thin-layer chromatography	< 0.22 mg/cm^3
Radiochemical purity of ^{18}F in the form of 2-[^{18}F]FDG and 2-[^{18}F]FDM*	Thin-layer chromatography	97 %–99 %
Glucose concentration	Liquid chromatography	0.0762 mg/cm^3
Acetonitrile concentration	Gas chromatography	0.03 mg/cm^3
Ethanol concentration	Gas chromatography	0.037 mg/cm^3

* 2-[^{18}F]FDM = 2-deoxy-2-[^{18}F]fluoro-D-mannose.

(removed root system by cutting with a scalpel blade) in small plastic vials containing of 2-[^{18}F]FDG solution with known specific ^{18}F radioactivity and composition in the given volume (see Table 1). To avoid spillage and evaporation of the solution, the plastic vials were covered with parafilm over the neck of the vial. In the second type of the experiments, the uptake of 2-[^{18}F]FDG was analyzed in the opposite (basipetal) direction as in the first type of experiments. The absorption of 2-[^{18}F]FDG by giant reed plants was realized through the leaf blade (excised using a scalpel in the middle part of the leaf) and by immersion of cut area of the leaf of whole plant into a 2-[^{18}F]FDG solution (see Table 1). Simultaneously, the root system of giant reed plant was immersed in a 25 % Hoagland medium without addition of 2-[^{18}F]FDG. The plant exposure and PET analyses were carried out during 120 min under laboratory conditions (temperature between 23–25 °C and a relative humidity of 40–45 %). At the end of the exposure period, the root system or immersed plant part were washed with deionised water to remove any unabsorbed 2-[^{18}F]FDG. The plants were then carefully placed on the scanning bed of the microPET system eXplore Vista pre-clinical PET scanner (GE Healthcare, Spain) and gently fixed with strips of parafilm. Acquisition of primary data was carried out in a static mode during 2 min for every length of the scanning bed position (2 cm). The total number of scanning bed positions was chosen depending on the length of the analyzed giant reed plant. The existence of stray signals originating from escaping positrons annihilated in the plastic material of the commercial scanning bed, was eliminated by the replacement of commercial scanning bed with a cardboard plate which showed a low ability to annihilate escaping positrons.

The used microPET system consists of 18 detection modules, whereby modules were arranged in a circle and the diameter of the ring was 11.8 cm. Each detection module was represented by 13 × 13 arrays of 1.45 mm × 1.45 mm × 7.0 mm lutetium oxyorthosilicate (LSO) crystals and 1.45 mm × 1.45 mm × 8.0 mm gadolinium orthosilicate single (GSO) crystals and was placed in time coincidence with the seven opposite modules to give an effective transverse field-of-view of 6.7 cm and an axial field-of-view of 2.0 cm. The performance capabilities of the microPET system used showed a reconstructed central spatial resolution of 1.5 mm, and the absolute central point source sensitivity was 1.9 % for the 250–700 keV energy window (required in this study).

For the control of microPET system, the acquisition of primary data, as well as the reconstruction of PET images (voxel size 0.3875 mm ×

0.3875 mm × 0.775 mm) the program eXplore VISTA ver. 3.1 (GE Healthcare, Spain) was used. The process of reconstruction involved the conversion of acquired 3D data sets to 2D sinograms with the Fourier rebinning (FORE) algorithm and the reconstruction of 2D sinograms with a 2D ordered subset expectation maximization (2D OSEM) reconstruction algorithm as well. Within the reconstruction process, the 2D sinograms were also corrected for accidental coincidences, radioactive decay and dead-time. The quality of visualization of regions with relatively lower accumulated radioactivity in reconstructed PET images was enhanced by adjusting the threshold using the program Amide.exe ver. 1.0.4.

Gamma-spectrometric analysis

For the precise determination of ^{18}F radioactivity accumulated in the individual parts of giant reed plants, a well-type scintillation detector assembled with a NaI(Tl) crystal (54BP54/2; Scionix, The Netherlands) and ScintiVision-32 software (Ortec, USA) were used. A library of radionuclides was built from characteristic γ-ray peaks of ^{109}Cd (E_γ = 88.04 keV), ^{18}F (E_γ = 511.00 keV) and ^{137}Cs (E_γ = 661.66 keV) for the energy and efficiency calibration. The radioactivity of individual samples was corrected on the basis of the ^{18}F half-life ($T_{1/2}$ = 109.5 min) to the time of PET analysis completion. Higher values of ^{18}F radioactivity (> 1.10^5 Bq) of applied 2-[^{18}F]FDG solutions or samples of individual parts of giant reed plants were also analyzed by ionisation chamber (Curiementor; 3PTW, Germany).

Results and Discussion

Giant reed plants have not yet been studied using non-invasive imaging techniques, such as positron emission tomography (PET). Previously, Hattori *et al.* (2008) and Karve *et al.* (2015) applied the PET in the analysis of the uptake and distribution of radioindicator in the tissues of sorghum (*Sorghum bicolour* L.) plants also belonging to *Poaceae* like giant reed plants.

In this work, we evaluated the possibility to visualize and quantify the uptake and distribution of 2-[^{18}F]FDG, as a model of photoassimilates, in tissues of giant reed (*A. donax* L. var. *versicolor*) plants using positron emission tomograph. The processes of absorption of 2-[^{18}F]FDG and its subsequent transport in the tissues of giant reed plants were analyzed in acropetal and basipetal direction as well. Moreover, in acropetal mode of 2-[^{18}F]FDG transport, the role of root system, as a natural selective barrier determining the solute transport, was also studied in the case of mechanically damaged root system (cut root capillaries) or removed root system. To obtain the visual as well as quantitative data, the positron emission tomograph primarily developed for animal objects and direct gamma-spectrometry were used. In the PET analysis, the process of visualization and quantification of accumulation of ^{18}F radioactivity in the form of 2-[^{18}F]FDG in the plant tissues included the measurements of the number of true coincidences (Num_C) corresponding to two gamma quantum of 511 keV emitted under 180° with respect to each other by annihilation of positron and negatron.

In the first series of experiments, we focused on studying and comparison of the distribution and accumulation of ^{18}F radioactivity in the form of 2-[^{18}F]FDG in tissues of giant reed plants after 120 min of their exposure by immersion with the intact root system, damaged root system or stem into a 2-[^{18}F]FDG solution with known ^{18}F radioactivity and D-glucose concentration. Individual parts of plants were distributed within the 9 (Fig. 1A), 12 (Fig. 1B) or 11 (Fig. 1C) scanning bed positions (1 bed position = 2 cm of axial length), where the first positions represent the root system or immersed part of the stem and the last positions represent the topmost leaves. Initial conditions of experiments and obtained data from PET analysis of giant reed plants are summarized in Table 2.

The obtained PET images depicted in the Fig. 1A show that the applied 2-[^{18}F]FDG was minimally translocated from the intact root system to the non-immersed parts of plant. Measurements of Num_C confirmed that up to 91 % of detected ^{18}F

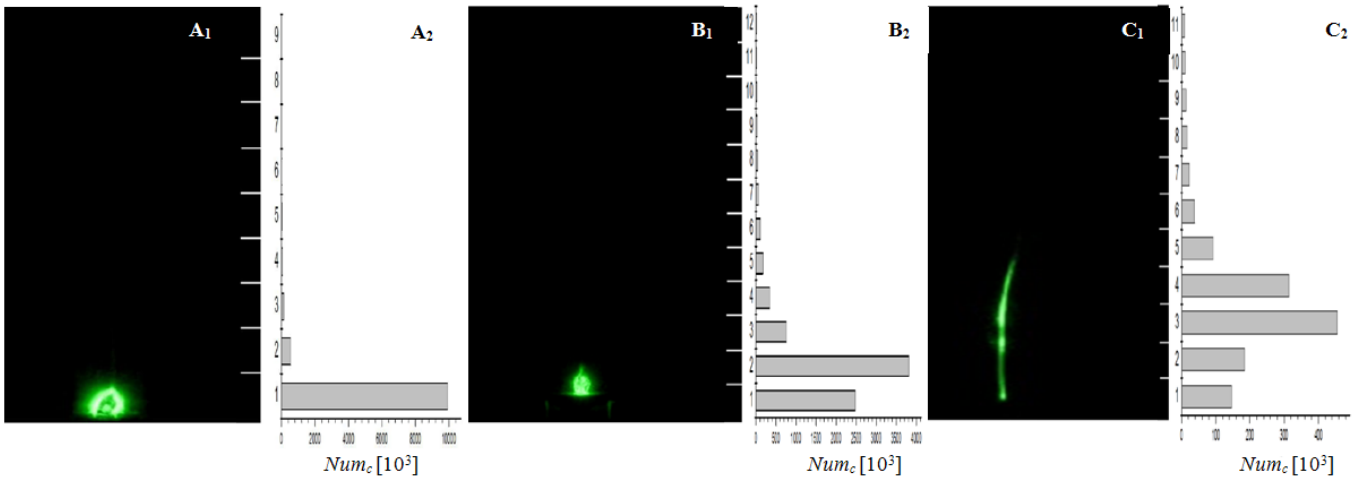

Fig. 1. Visualisation of 2-[^{18}F]FDG distribution in tissues of giant reed plants (*A. donax* L. var. *versicolor*) analysed by microPET system after 120 min of exposure of the plant immersed with the intact root system (**A**), damaged root system (**B**; cut root capillaries) or stem (**C**; removed root system by cutting with a scalpel blade) into a 2-[^{18}F]FDG solution (initial radioactivity 80 MBq) containing 0.00762 mg/cm^3 of D-glucose. The acquisition time (2 min/bed position) was: A. 18 min for 9 scanning bed positions; B. 24 min for 12 scanning bed positions; C. 22 min for 11 scanning bed positions. Index **1** – PET image; Index **2 –** The number of analysed coincidences (*Num$_C$*) within the PET analysis of plant for individual scanning bed positions.

Table 2. Initial conditions of experiments and obtained data from PET analysis of giant reed plants (*A. donax* L. var. *versicolor*) after the exposure of individual parts of plant in a 2-[^{18}F]FDG solution. For details see Fig. 1 and 2.

Parameter	**Uptake of 2-[^{18}F]FDG by root**	**Uptake of 2-[^{18}F]FDG by damaged root**	**Uptake of 2-[^{18}F]FDG by stem**	**Uptake of 2-[^{18}F]FDG by cut leaf**
m_P (g; w.w.)	0.321	0.453	0.379	3.63
A_0 (MBq)	80	80	80	274
Num$_C$	10,762	7,869	1,301	3,526
EV (cm^3)	3.53	2.19	1.02	60.1
PV	30,316	18,811	8,753	516,000
TGV	38,818*10^3	24,630*10^3	3,977*10^3	10,759*10^3
MaxPV	33,012	59,934	17,376	1,050
TFc	0.084	0.251	2.93	–

m_P – fresh weight of the plant (g); A_0 – initial applied radioactivity of 2-[^{18}F]FDG solution (MBq); *Num$_C$* – number of analysed coincidences within the PET analysis; *EV* – estimated volume within the PET analysis (cm^3); *PV* – pixel volume; *TGV* – total gray value; *MaxPV* – maximum pixel value; *TFc* – coincidence transfer factor defined as the ratio of the *Num$_C$* in the non-immersed parts of the plant to the *Num$_C$* in the parts of the plant immersed into a 2-[^{18}F]FDG solution.

coincidences correspond to the accumulated radioactivity in the intact root system. A similar result was described by Partelová *et al.* (2014) for the 2-[^{18}F]FDG uptake in whole tobacco plants. These authors found that a significant part of the accumulated ^{18}F radioactivity was allocated in the root system of tobacco, while a minimal transport of 2-[^{18}F]FDG into the aboveground parts was observed. This result can be explained by the fact that the natural role of the root system is to form a selective barrier for the transport of substances from the roots to the aerial parts of plant. According to Fatangare and Svatoš (2016), this barrier is likely to constitute by Casparian strips in the radial and transverse cell walls of the endodermis. Partelová *et al.* (2014) also found that on the quantitative side of the 2-[^{18}F]FDG transport from the root system to the aerial parts of plant, the concentration of D-glucose as a carrier will play a decisive role.

To eliminate the function of root system as a selective barrier of solute transport,

in the second type of the experiment about half of the root system was removed by cutting the root capillaries (damaged root system) prior to the immersion into a 2-[^{18}F]FDG solution. By this root treatment, we expected the reduction of the surface of the root system as an area with enhanced 2-[^{18}F]FDG accumulation and the suppression of the activity of Casparian strips as well. We found that the 2-[^{18}F]FDG was minimally translocated from the immersed root to the non-immersed parts of plant (to stems or leaves) (Fig. 1B), but in a higher extent than in the first type of the experiment (Fig. 1A). In the damaged root system of giant reed plants, approx. 75 % of analyzed ^{18}F coincidences from the total accumulated radioactivity were measured. Fatangare *et al.* (2014) also studied the uptake and distribution of 2-[^{18}F]FDG in tissues of *Arabidopsis thaliana* plants by combined positron emission tomography with computed tomography (PET/CT). Their results showed a comparable proportion of ^{18}F radioactivity accumulated in the aboveground plant parts to the accumulated radioactivity in the root system, whereby the highest specific radioactivities were mainly analyzed in the nodal stems and root system. According to values of coincidence transfer factor TF_C (Table 2), it was found that approx. 4-fold higher amount of 2-[^{18}F]FDG was accumulated in damaged root system than in the aboveground parts of plant (TF_C = 0.25) and approx. 12-fold higher amount of 2-[^{18}F]FDG was accumulated in the intact root system (TF_C = 0.08) under the same experimental conditions. Thus, damaging the root system caused a 3-fold increase in the translocation of 2-[^{18}F]FDG into the aerial parts of giant reed plant in comparison with the plant immersed into a 2-[^{18}F]FDG solution by intact root system. In general, a very low level of 2-[^{18}F]FDG translocation into leaves can be related to low transpiration rate of giant reed plants (found by independent experiments).

In the last type of the experiment, the uptake and transport of 2-[^{18}F]FDG were evaluated for giant reed plant without root system with the aim to confirm the role of the root and the function of Casparian strips as selective barriers controlling the 2-[^{18}F]FDG transport into aboveground parts of plant. Fig. 1C shows that root system removal resulted in enhanced distribution of 2-[^{18}F]FDG along the stem, probably due to capillary action of water in the xylem pathway. As in the case of previous experiments, the visually evaluable PET image in terms of visualization of 2-[^{18}F]FDG distribution within the whole plant body was not obtained. This fact can be related with the formation of "hot spots" representing high levels of specific radioactivity accumulated in individual plant parts (e.g. root or stem segments) that represent problems in the detection of relatively low levels of radioactivity in other parts of the plant. This phenomenon could be explained by the technical nature and performance characteristics of PET systems, which are designed to accurately visualize regions with high accumulation of radioactivity and reject regions with low accumulation of radioactivity. However, it was found that approx. 3-times higher ^{18}F radioactivity was analyzed in the non-immersed parts of plant than radioactivity accumulated in stem (TF_C = 2.93). The significant 2-[^{18}F]FDG accumulation in the leaves was also verified and confirmed by direct gamma-spectrometry. The highest ^{18}F radioactivity (Bq) value was detected in the case of young developed leaves (data not shown). In relation to this finding, it is interesting that despite of high ^{18}F radioactivity accumulated in young developed leaves these regions were not visualized within the PET record. Contrary to this finding, the stem showing a slightly lower accumulation of ^{18}F radioactivity was visualized in obtained PET image. This fact can be explained by different specific ^{18}F radioactivities (in Bq/cm^2 for 2D PET image or Bq/cm^3 for 3D PET image) accumulated in individual plant parts, when the highest specific ^{18}F radioactivities are allocated in stem as area and volume smaller objects than leaves. Therefore, the regions with the highest specific ^{18}F radioactivities are visualized in PET images, but the regions with lower specific ^{18}F radioactivities are eliminated within the reconstruction of PET images. In the second series of experiments, the uptake and transport of 2-[^{18}F]FDG were

analyzed in basipetal direction, when the plant was exposed to the 2-[^{18}F]FDG solution through the cut area of the leaf (in the middle part of the leaf).

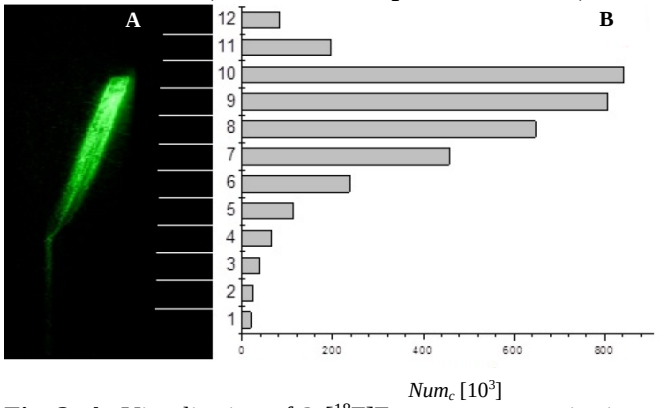

Fig. 2. A. Visualisation of 2-[^{18}F]FDG distribution in tissues of giant reed plant (*A. donax* L. var. *versicolor*) analysed by microPET system after 120 min of exposure of the plant immersed with the cut area of the leaf (in the middle part of the leaf) of whole plant into a 2-[^{18}F]FDG solution (initial radioactivity 274 MBq) containing 0.00762 mg/cm^3 of D-glucose. Simultaneously, the root system of giant reed plant was immersed in a 25 % Hoagland medium without addition of 2-[^{18}F]FDG. The acquisition time was 24 min for 12 scanning bed positions (2 min/bed position). **B.** The number of analysed coincidences (*Num$_C$*) within PET analysis of plant for individual scanning bed positions.

In the literature focused on the analysis of uptake and translocation of compounds in plant tissues using PET, the application of radiotracer on the cut leaf tip of plants represents a relatively common method. For example, Hattori *et al.* (2008) using this approach found that 2-[^{18}F]FDG was uptaken from the leaf tip and it wastranslocated to the basal part of the shoots from where it moved further to the roots, the tillers and the sheaths of sorghum plant. As it can be seen in the Fig. 2, the immersion of cut leaf in our study did not resulted in significant translocation of 2-[^{18}F]FDG into the other plant parts. Initial conditions of experiment and obtained data from PET analysis are presented in the Table 2. We suppose a more significant translocation of 2-[^{18}F]FDG into other plant parts would require a longer-term exposure, but the application of ^{18}F as a positron emitter with short half-life decay ($T_{1/2}$ = 109.5 min) is a limiting factor in this way. Previously, Partelová *et al.* (2016) have explained a fast initial uptake of 2-[^{18}F]FDG in tobacco leaves through the cut petiole as a result of physico-chemical process driven by capillary action of water in the xylem pathway. Fatangare *et al.* (2015) have noted that 2-[^{18}F]FDG as a radioactive analogue of D-glucose can also be transported by phloem, while the behaviour and metabolism of 2-[^{18}F]FDG in plant tissues remain still unclear. The distribution of ^{18}F radioactivity in giant reed plant after the 2-[^{18}F]FDG administration through the cut leaf was also analyzed by direct gamma-spectrometry (Fig. 3). Obtained results are in agreement with the PET analysis. It was confirmed that more than 98 % of ^{18}F radioactivity accumulated by plant was allocated in the immersed cut leaf. Also, the translocation of 2-[^{18}F]FDG in the direction of the root system represents a more likely process than the translocation of 2-[^{18}F]FDG in the direction of topmost leaves (Fig. 3B).

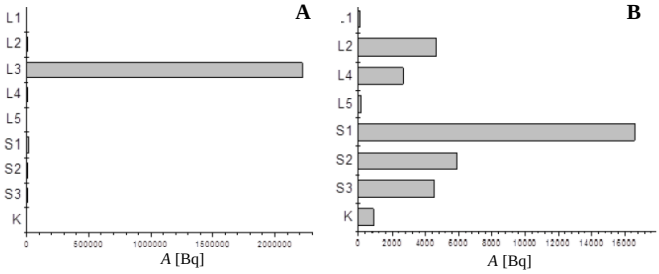

Fig. 3. A. ^{18}F radioactivity analysed in individual parts of giant reed plant (*A. donax* L. var. *versicolor*) by direct gamma-spectrometry. For details of experiments see Fig. 2. The numbering of leaves (L): 1. the oldest developed leaf, 5. the youngest developed leaf, 3. exposed leaf immersed into a 2-[^{18}F]FDG solution; and stem (S): 1. lower stem, 3. top stem; K – root system. **B.** Detailed distribution of ^{18}F radioactivity analysed in individual parts of giant reed plant without exposed leaf L3.

Conclusions

The obtained results show that commercial microPET systems primarily developed for animal objects and 2-deoxy-2-fluoro[^{18}F]-D-glucose (2-[^{18}F]FDG) can be used for analysis of whole-plant photoassimilates allocation in energy crops. Visualization and quantification of the uptake and transport of 2-[^{18}F]FDG in giant reed plant immersed with the root system into a 2-[^{18}F]FDG solution revealed a significant accumulation of ^{18}F radioactivity in the roots, confirming the natural function of this organ as a selective barrier determining the solute transport. The 2-[^{18}F]FDG transport expressed as coincidence transfer factor

TF_C = $[^{18}F]_{non\text{-}immersed\ plant\ part}$: $[^{18}F]_{immersed\ plant\ part}$ was increased in the order of plant exposure through: stem (removed root system by cutting with a scalpel blade) > mechanically damaged root system (cut root capillaries) > intact root system. Thus, the complete removal of the root system with Casparian strips as selective barriers of solute transport into the aboveground parts of plant caused a significant increase in 2-[^{18}F]FDG allocation into the aerial parts of giant reed plants, especially into the young developed leaves. PET analysis of the uptake and transport of 2-[^{18}F]FDG in basipetal direction, when the plant was immersed with the cut area of the leaf of whole plant into a 2-[^{18}F]FDG solution, showed minimal translocation of 2-[^{18}F]FDG into the other plant parts. However, it was found that the translocation of 2-[^{18}F]FDG from the cut leaf into the root system represents a more likely process than the translocation of 2-[^{18}F]FDG in the direction of topmost leaves.

The possibility of visualization and quantification of carbon allocation or photoassimilate transport dynamics under *real-time* and *in vivo* conditions can be important for functional genomic studies to reveal the mechanisms controlling their allocation and transport in energy crops, which will provide crucial insights for improving yields. However, as was demonstrated in this study, the physical properties of positron-emitting isotopes, performance characteristics or capabilities of PET systems as well as the design of experiments can restrict the PET application in plant biology.

Acknowledgement

This work was supported by the Slovak Research and Development Agency under the contract No. APVV-15-0098. Financial support for the stay of Yevheniia Konotop at UCM in Trnava is provided by Slovak Academic Information Agency (SAIA).

References

Czakó M, Márton L (2010) Subtropical and tropical reeds for biomass. *In:* Halford NG, Karp A (Eds.), Energy crops, RSC Publishing, Cambridge, UK: 322-340.

Evans JR (2013) Improving photosynthesis. Plant Physiol. 162: 1780-1793.

Fatangare A, Gebhardt P, Saluz H, Svatoš A (2014) Comparing 2-[^{18}F]fluoro-2-deoxy-D-glucose and [^{68}Ga]gallium-citrate translocation in *Arabidopsis thaliana*. Nucl. Med. Biol. 41: 737-743.

Fatangare A, Paetz C, Saluz H, Svatoš A (2015) 2-deoxy-2-fluoro-D-glucose metabolism in *Arabidopsis thaliana*. Front. Plant Sci. 6: 935.

Fatangare A, Svatoš A (2016) Applications of 2-deoxy-2-fluoro-D-glucose (FDG) in plant imaging: Past, present, and future. Front. Plant Sci. 7: 483.

Fiorani F, Rascher U, Jahnke S, Schurr U (2012) Imaging plants dynamics in heterogenic environments. Curr. Opin. Biotechnol. 23: 227-235.

Hattori E, Uchida H, Harada N, Ohta M, Tsukada H, Hara Y, Suzuki T (2008) Incorporation and translocation of 2-deoxy-2-[^{18}F]fluoro-D-glucose in *Sorghum bicolour (L.)* Moench monitored using a planar positron imaging system. Planta 227: 1181-1186.

Hoagland DR (1920) Optimum nutrient solution for plants. Science 52: 562-564.

Hubeau M, Steppe K (2015) Plant-PET scans: *In vivo* mapping of xylem and phloem functioning. Trends Plant Sci. 20: 676-685.

Kawachi N, Yin Y-G, Suzui N, Ishii S, Yoshihara T, Watabe H, Yamamoto S, Fujimaki S (2016) Imaging of radiocesium uptake dynamics in a plant body by using a newly developed high-resolution gamma camera. J. Environ. Radioact. 151: 461-467.

Karve AA, Alexoff D, Kim D, Schueller MJ, Ferrieri RA, Babst BA (2015) *In vivo* quantitative imaging of photoassimilate transport dynamics and allocation in large plants using a commercial positron emission tomography (PET) scanner. Plant Biol. 15: 273.

Kiser MR, Reid CD, Crowell AS, Phillips RP, Howell CR (2008) Exploring the transport of plant metabolites using positron emitting radiotracers. HFSP J. 2: 189-204.

Mack RN (2008) Evaluating the credits and debits of a proposed biofuel species: giant reed (*Arundo donax*). Weed Sci. 56: 883-888.

McRae R, Bagchi P, Sumalekshmy S, Fahrni CJ (2009) *In situ* imaging of metals in cells and tissues. Chem. Rev. 109: 4780-4827.

Murashige T, Skoog F (1962) A revised medium for rapid growth and bio assays with tobacco tissue cultures. Physiol. Plant. 15: 473-497.

Partelová D, Uhrovčík J, Lesný J, Horník M, Rajec P, Kováč P, Hostin S (2014) Application of positron emission tomography and 2-[^{18}F]fluoro-2-deoxy-D-glucose for visualization and quantification of solute transport in plant tissues. Chem. Pap. 68: 1463-1473.

Partelová D, Horník M, Lesný J, Rajec P, Kováč P, Hostin S (2016) Imaging and analysis of thin structures using positron emission tomography: thin phantoms and *in vivo* tobacco leaves study. Appl. Radiat. Isot. 115: 87-96.

Pilu R, Bucci A, Badone FC, Landoni M (2012) Giant reed (*Arundo donax* L.): A weed plant or a promising energy crop? Afr. J. Biotechnol. 11: 9163-9174.

Plathow CH, Weber WA (2008) Tumor cell metabolism imaging. J. Nucl. Med. 49: 43S-63S.

Rossa B, Tuffers AV, Naidoo G, Von Willert DJ (1998) *Arundo donax* L. (*Poaceae*) – a C3 species with unusually high photosynthetic capacity. Bot. Acta. 111: 216-221.